M R S Internet Journal of Nitride Semiconductor Research

Volume 1, Article 30

Electronic structure of biaxially strained wurtzite crystals GaN, AlN, and InN

J. A. Majewski, M. Städele, P. Vogl
Walter Schottky Institut, Technische Universität München

This article was received on June 11, 1996 and accepted on October 31, 1996.

Abstract

We present first-principles studies of the effect of biaxial (0001)-strain on the electronic structure of wurtzite GaN, AlN, and InN. We provide accurate predictions for the valence band splittings as a function of strain which greatly facilitates the interpretation of data from samples with unintentional growth-induced strain. The present calculations are based on the total-energy pseudopotential method within the local-density formalism and include the spin-orbit interaction nonperturbatively. For a given biaxial strain, all structural parameters are determined by minimization of the total energy with respect to the electronic and ionic degrees of freedom. Our calculations predict that the valence band state Γ_9 (Γ_6) lies energetically above the Γ_7 (Γ_1) states in GaN and InN, in contrast to the situation in AlN. In all three nitrides, we find that the ordering of these two levels becomes reversed for some value of biaxial strain. In GaN, this crossing takes place already at 0.32% tensile strain. For larger tensile strains, the top of the valence band becomes well separated from the lower states. The computed crystal-field and spin-orbit splittings in unstrained materials as well as the computed deformation potentials agree well with the available experimental data.

1. Introduction

The group-III nitrides AlN, GaN, and InN have recently attracted much attention as candidates for short-wavelength optical devices [1]. The stable structure of bulk materials is the wurtzite structure. For technological applications, one needs high quality epitaxial films that are presently grown mostly on c-plane sapphire or hexagonal 6H-SiC substrates and also possess the wurtzite structure. The large lattice mismatch between the mentioned substrates and the nitrides induces a substantial strain in the latter materials. Even though the largest part of this strain seems to be relieved by generation of misfit dislocations, another strain contribution comes from the difference in the thermal expansion coefficients between the substrates and the nitrides. In result, an appreciable growth-induced biaxial strain remains in the nitride films that is very difficult to measure experimentally in a direct way. On the other hand, optical excitation energies of these films are well accessible experimentally.

In this paper, we provide quantitative theoretical predictions of the major optical transitions across the energy gap of group-III nitrides as a function of biaxial strain that may help determining the actual strain in epitaxial films from optical data.

The band structure of bulk AlN, GaN, and InN in the wurtzite and zinc-blende phase has been extensively studied theoretically [2]. However, few reports have dealt with strain effects so far. In Refs. [3], [4], the effects of strain on the band structure of cubic GaN were studied. An interesting qualitative discussion of the effects of biaxial strain on cubic and hexagonal GaN in terms of a simple tight-binding model was given in Ref. [5].

In the wurzite structure, the top of the valence band is split into three states that give rise to three corresponding exciton lines. In GaN, these exciton energies were recently measured as a function of the film thickness [6], [7], i.e. effectively as a function of strain, but the authors have not been able to determine the magnitude of the strain experimentally.

Employing parameter-free, relativistic local density functional pseudopotential methods, we have analyzed the

https://doi.org/10.1557/S1092578300002027 Published online by Cambridge University Press

electronic band energies of three wurtzite structure nitrides as a function of biaxial and hydrostatic strain in order to provide a link between optical data and the effective strain. From a theory point of view, it turned out to be crucial to fully optimize all structural parameters that are not determined by symmetry and to take into account spin-orbit coupling in order to resolve the fine structure of the band edge states and the interplay between spin-orbit interaction and strain in these materials.

2. Method and numerical aspects

Our calculations are based on the first-principles total-energy pseudopotential method within the local-density-functional formalism [8]. We have used norm-conserving separable pseudopotentials [9], [10] and a preconditioned conjugate gradient algorithm [11] for minimizing the total crystal energy with respect to the electronic as well as the ionic degrees of freedom. These pseudopotentials are highly transferable, yet sufficiently soft so that a kinetic energy cutoff of 62 Ry suffices to yield converged total energies. We have used 14 special points [12] for the k-space integrations. The semicore Ga 3d-electrons are treated as part of the frozen core, but their considerable overlap with the valence electrons is accounted for by including the nonlinear core exchange-correlation correction [13]. This procedure yields lattice constants, atomic positions, and bulk moduli in very good agreement with experiment, as shown in Table 1. In order to realistically account for the interplay between strain and spin-orbit-interaction induced valence band splittings, in the present calculations we have taken into account relativistic effects nonperturbatively by using relativistic pseudopotentials. This method has been shown to predict spin-orbit splittings in other III-V compounds very reliably [14].

3. Results

3.1. Structural optimization

On the scale of meV, the energy bands near the energy gap depend critically on those wurzite structural parameters that are not determined by symmetry. We have therefore performed detailed structural optimizations of the unit cell geometries as a function of the external stress by minimizing the total energy.

In the case of hydrostatic pressure or biaxial stress, the wurzite structure has two degrees of freedom, namely the ratio of lattice constants c/a and the bond length d along the hexagonal axis (0001). This defines a parameter u via the relation d = u c. For the ideal unstrained wurzite structure, one has u = 0.375. In spite of the fact that the calculated structural parameters in Table 1 are close to this ideal ratio, the deviations from this ratio alter the valence band splittings by more than 100%. The energy difference between the topmost valence bands at Γ (crystal field splitting) in unstrained GaN and AlN equals 35 meV and -211 meV, respectively, for the optimized values of u (Table 1) instead of 70 meV and -55 meV, respectively, as obtained with the ideal value u=3/8 (see also [15]). Thus, accurate structural optimizations are mandatory for predicting fundamental optical transitions in these materials.

We now wish to discuss the band structure of strained nitrides. We have determined the parameters c and u for both small biaxial strain in the (0001) plane and hydrostatic strain as a function of the lateral lattice constant a. For these types of strain, the strain tensor has only diagonal matrix components $e_{xx} = e_{yy} = e_{//} = a/a_0 - 1$, $e_{zz} = (c/c_0 - 1)$ (a_0, c_0 denote the equilibrium lattice constants). The present ab-initio calculations predict $e_{zz} = \sigma e_{//}$, with σ equal to -0.4567 (1.0143), -0.5719 (1.1922), and -0.7926 (1.1740) for GaN, AlN, and InN, respectively. The negative values are for biaxial strain, whereas the positive ones in parenthesis are for the case of hydrostatic pressure.

3.2. Three-band k·p Hamiltonian for strained valence band edge energies

Our calculations confirm that all three studied compounds are indeed direct gap semiconductors in the wurtzite structure with the fundamental gap located at the Γ point ($\mathbf{k} = 0$) [1]. The valence band edge states in the strained wurzite structure near $\mathbf{k}$=0 can be represented by a 6 x 6 k·p Hamiltonian [16]. Interestingly, this 6 x 6 matrix can be diagonalized analytically for $\mathbf{k} = 0$ and biaxial strain or hydrostatic pressure. The energy eigenvalues, relative to their center of gravity, can be written in the form [17]

$$E(\Gamma_{9v}) = (1/3)(\Delta_1 + \Theta(\mathbf{e})) + \Delta_2 \quad (1)$$

$$E_{\pm}(\Gamma_{7v}) = (-1/6)(\Delta_1 + \Theta(\mathbf{e})) + (1/2)\{-\Delta_2 \pm ((\Delta_1 + \Theta(\mathbf{e}) - \Delta_2)^2 + 8\Delta_3^2)^{1/2}\}, \quad (2)$$

https://doi.org/10.1557/S1092578300002027 Published online by Cambridge University Press

$$\Theta(\mathbf{e}) = D_3\, e_{zz} + 2\, D_4\, e_{//}, \qquad (3)$$

where the constants D_3 and D_4 are deformation potentials and Δ_2 and Δ_3 are spin-orbit coupling constants. In the absence of spin-orbit interaction and for zero strain, one has $E(\Gamma_{9v}) = E_+(\Gamma_{7v}) = \Delta_1/3$, $E_-(\Gamma_{7v}) = -2\Delta_1/3$. Depending on the sign of Δ_1, the top of the valence band is formed by the $E(\Gamma_{9v})$ state (as in GaN, InN) or the $E_+(\Gamma_{7v})$ state (as in AlN). Therefore, Δ_1 is conventionally termed crystal-field splitting. Let us point out that we have set to zero the average valence band energy since we are only interested in optical excitation energies. The term $\Theta(\mathbf{e})$ represents the strain dependence of the crystal field splitting. We also note that this k·p Hamiltonian neglects the influence of strain on the spin-orbit coupling constants.

The shift of the conduction band edge at Γ with strain is governed by two deformation potentials A_1 and A_2: $E(\Gamma_{7c}) = E(\Gamma_{7c}; \mathbf{e} = 0) + A_1\, e_{zz} + 2\, A_2\, e_{//}$. Because of the degeneracy of the valence band edge, it is more transparent to measure this strain dependence relative to the center of gravity of the valence band rather than focusing directly on the strain dependence of the gap.

3.3. Validity of linear strain approximation

We have used the results of the ab-initio calculations to determine the valence band parameters Δ_i and deformation potentials D_i and A_i. In order to determine Δ_1 independently from Δ_2, Δ_3 and separate the strain and relativistic effects from each other, we have also performed nonrelativistic pseudopotential calculations. We find that the numerically determined valence band eigenvalues can be well represented in terms of the model discussed above, provided the strain tensor elements lie in the range of $|e_{ij}| < 0.01$ for biaxial strain and $|e_{ij}| < 0.04$ for hydrostatic deformation. In the case of larger biaxial strains, $\Theta(\mathbf{e})$ shows pronounced nonlinearities. For biaxial strains between 0.01 and 0.04, the discrepancies between the numerical eigenvalues and the eigenvalues given in Equation 1-Equation 3 stem from the nonlinear strain dependence of $\Theta(\mathbf{e})$, whereas the spin-orbit interaction parameters are independent of strain in this range.

For a given external biaxial or hydrostatic stress, the total energy minimization relates the strain tensor component $e_{//}$ to e_{zz}. In order to determine both pairs of deformation potentials D_3,D_4 and A_1, A_2, therefore we have computed $(d\Theta(\mathbf{e})/de_{//})_{\mathbf{e}=0}$ and $(dE_{gap}(\mathbf{e})/de_{//})_{\mathbf{e}=0}$ both for biaxial strain as well as for hydrostatic pressure. This gives, for each set of deformation potentials, 2 linear equations for the 2 unknowns. One should notice however, that in the case of small gap semiconductor as InN (in our LDA calculations the energy gap equals 0.1 eV in unstrained wurtzite InN) the description of the valence band through the six band model is doubtful. Therefore, the determined valence band parameters for InN have plausibly no physical meaning and they should be treated as formal parameters that reproduce the theoretical valence band splittings and their derivatives with the strain.

3.4. Valence band parameters and deformation potentials

The predicted valence band parameters are summarized in Table 2. The strained valence band eigenvalues as obtained from the full relativistic LDA calculations are depicted in Figure 1. We have compared them with the energies obtained from the model Equation 1-Equation 3 with the parameters from Table 2. As discussed above, the agreement between LDA calculations and the analytic expressions is excellent for moderate strains. For larger strains the discrepancy increases, due to the nonlinearity of $\Theta(\mathbf{e})$, but it remains acceptable for strains up to 3%. For unstrained GaN, the present ab-initio calculations predict $E(\Gamma_{9v}) - E_+(\Gamma_{7v}) = 8$ meV (6 meV [7], [18] , [19], [20]) and $E(\Gamma_{9v}) - E_-(\Gamma_{7v}) = 43$ meV (22 meV [7], 18 meV [18], 28 meV [19], 24 meV [20]), in fair agreement with the experimental data (in parenthesis) of thin GaN films.

Figure 1 reveals that the energetic ordering of the $E(\Gamma_{9v})$ and $E_+(\Gamma_{7v})$ states changes beyond some critical value of biaxial strain. For GaN and InN, this occurs for 0.32% and 0.37% tensile strain, respectively, whereas in AlN a compressive strain of 1.56% is required.

From the results given in Table 2, one can determine the strain dependence of the energy gap. We find $dE_{gap}/de_{//} = -6.1$ eV (corresponding to 17.4 meV/GPa) for biaxial strain up to 0.32%, and -16 eV for tensile strain larger than 0.32%. This computed values agree very well with the experimental values -8.2 eV [7] and 24±4 meV/GPa [21] for compressive strain and -13 eV for tensile strain [7]. Additionally, we find very good agreement between the predicted and experimental value of the band gap pressure coefficient in GaN, $dE_{gap}/dp = 40.1$ meV/GPa (exp: 41 meV/GPa [22], 42 meV/GPa [23]).

https://doi.org/10.1557/S1092578300002027 Published online by Cambridge University Press

In the case of InN, the spin-orbit coupling constants obtained in our pseudopotential calculations (Δ_2 = 3.9 meV and Δ_3 = 5.5 meV) are only moderately smaller than spin-orbit splittings in AlN and GaN (see Table 1). It is in contrast to the recent all-electron calculations, which predict the value of the spin-orbit splitting Δ_0 in the zincblende InN to be 3 meV [24] and 6 meV [25] (please note that in the cubic model of wurtzite structure $\Delta_2 = \Delta_3 = \Delta_0/3$).

In summary, we have predicted the strain dependence of the valence band edge states of wurzite GaN and AlN. We have developed an analytical model for these electronic energies that accurately reproduces the complex interplay between spin-orbit and strain effects.

Acknowledgments

This work was supported by the Bayerische Forschungsverbund FOROPTO and the Deutsche Forschungsgemeinschaft, project SFB 348.

References

[1] S. Strite, H. Morkoç, *J. Vac. Sci. Technol. B* ***10***, 1237-1266 (1992).

[2] JH Edgar, (Editor), *Properties of Group III Nitrides* (Electronic Materials Information Service (EMIS), London, 1994) .

[3] Kwiseon Kim, Walter R. L. Lambrecht, Benjamin Segall , *Phys. Rev. B* ***50***, 1502-1505 (1994).

[4] J Xie, J Zi, K Zhang, *Phys. Stat. Sol. B* ***192***, 95-100 (1995).

[5] M Nido, *Jpn. J. Appl. Phys.* ***34***, L1513-L1516 (1995).

[6] B Gil, O Briot, RL Aulombard, *Phys. Rev. B* ***52***, R17028-17031 (1995).

[7] D Volm, K Oettinger , T Streibl , D Kovalev , M Ben-Chorin, J Diener , BK Meyer , J Majewski, L Eckey , A Hoffman , H Amano , I Akasaki , K Hiramatsu , T Detchprohm, *Phys. Rev. B* ***53***, 16543-16550 (1996).

[8] WE Pickett, *Comp. Phys. Rep.* ***9***, 115-198 (1989).

[9] N Troullier, JL Martins, *Phys. Rev. B* ***43***, 1993-2006 (1991).

[10] L Kleinman, DM Bylander, *Phys. Rev. Lett.* ***48***, 1425-1428 (1982).

[11] MC Payne, MP Teter, DC Allan, TA Arias, JD Joannopoulos, *Rev. Mod. Phys.* ***64***, 1045-1097 (1992).

[12] PJH Denteneer, W Van Haeringen, *Sol. St. Comm.* ***59***, 829-832 (1986).

[13] SG Louie, S Froyen, ML Cohen, *Phys. Rev. B* ***26***, 1738-1742 (1982).

[14] JA Majewski, in *The Physics of Semiconductors*, Edited by: DJ Lockwood, (World Scientific, Singapore, 1995) 711-714.

[15] Masakatsu Suzuki, Takeshi Uenoyama , Akira Yanase , *Phys. Rev. B* ***52***, 8132-8139 (1995).

[16] G.L. Bir, G.E. Pikus, *Symmetry and strain-induced effects in Semiconductors* (John Wiley Sons, New York, 1974) .

[17] SL Chuang , CS Chang, *Phys. Rev. B* ***54***, 2491-2504 (1996).

[18] R. Dingle, D. D. Sell, S. E. Stokowski, M. Ilegems, *Phys. Rev. B* ***4***, 1211 (1971).

https://doi.org/10.1557/S1092578300002027 Published online by Cambridge University Press

[19] B. Monemar, *Phys. Rev. B* ***10***, 676 (1974).

[20] K Pakula, A Wysmolek, KP Korona, JM Baranowski, R Stepniewski, I Grzegory, M Bockowski, J Jun, S Krukowski, M Wroblewski, S Porowski, *Sol. St. Comm.* ***97***, 919-922 (1996).

[21] W Rieger, T Metzger, H Angerer, R Dimitrov, O Ambacher, M Stutzmann, *Appl. Phys. Lett.* ***68***, 970 (1996).

[22] D. L. Camphausen, G. A. N. Connell, *J. Appl. Phys.* ***42***, 4438 (1971).

[23] P. Perlin, I. Gorczyca , N. E. Christensen , I. Grzegory, H. Teisseyre, T. Suski , *Phys. Rev. B* ***45***, 13307-13313 (1992).

[24] W.R.L. Lambrecht, K. Kim , S. N. Rashkeev , B. Segall, *Mater. Res. Soc. Symp. Proc.* ***395***, 455-466 (1996).

[25] S.-H. Wei, A. Zunger, unpublished (1996).

[26] H. Schulz, K. H. Thiemann, *Sol. St. Comm.* ***23***, 815 (1977).

[27] Masaki Ueno, Minoru Yoshida, Akifumi Onodera , Osamu Shimomura, Kenichi Takemura , *Phys. Rev. B* ***49***, 14-21 (1994).

Table 1

Table 1: Predicted structural parameters. Values in parentheses are experimental data from Ref. [2] (for a_0 and c_0), Ref. [26] (u_0), and Ref. [27] (B_0).

	AlN	GaN	InN
a_0 (Å)	3.091	3.174	3.538
	(3.111)	(3.189)	(3.544)
c_0 (Å)	4.954	5.169	5.707
	(4.978)	(5.185)	(5.718)
u_0	0.3815	0.3768	0.3792
	(0.382)	(0.377)	-
B_0 (GPa)	205	196	146
	(208)	(237)	(125)

Table 2

Table 2: Predicted valence band parameters and deformation potentials

	AlN	GaN	InN
Δ_1(meV)	-210.7	35.3	27.8
Δ_2(meV)	6.6	5.3	3.9
Δ_3(meV)	6.7	6.7	5.5
D_3 (eV)	9.18	6.61	4.77
D_4 (eV)	-4.10	-3.55	-1.32
A_1 (eV)	-10.50	-9.96	-4.71
A_2 (eV)	-9.75	-7.01	-2.72

https://doi.org/10.1557/S1092578300002027 Published online by Cambridge University Press

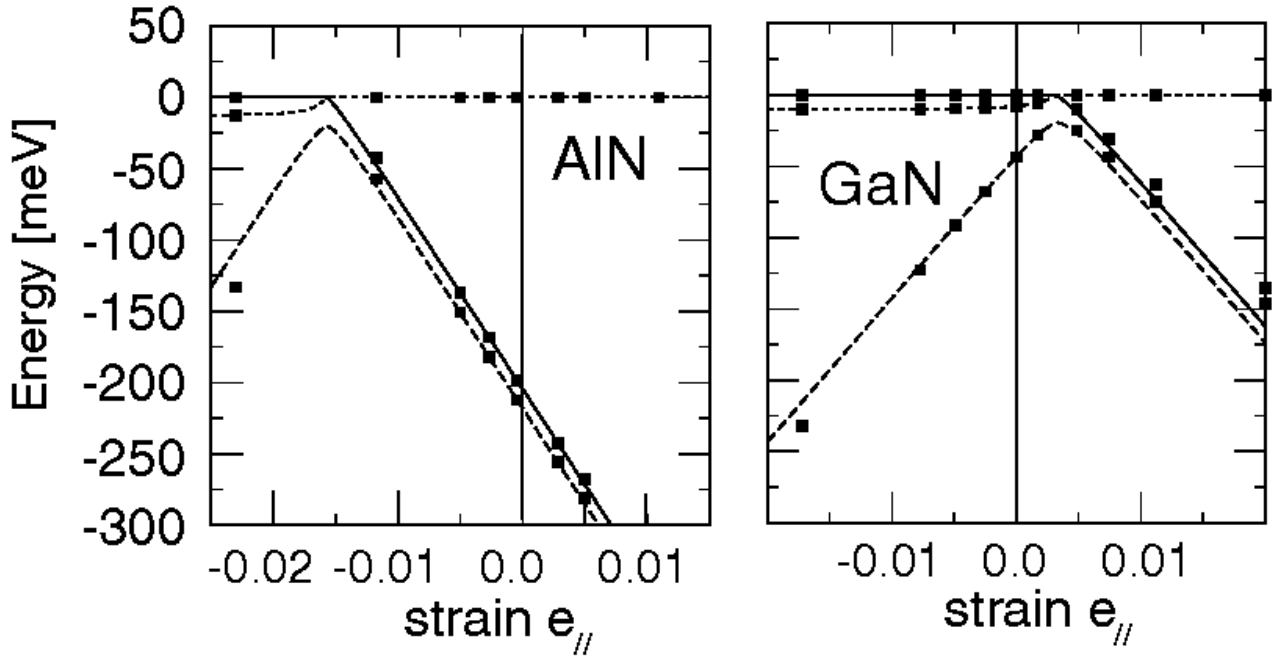

Figure 1. Calculated valence band energies of GaN and AlN (in meV) at Γ as a function of biaxial strain $e_{//}$. The top of the valence band is the zero of energy. The lines represent the energies of the analytical model from Equation 1-Equation 3 (full: $E(\Gamma_{9v})$, dotted: $E_+(\Gamma_{7v})$, dashed: $E_-(\Gamma_{7v})$) with parameters from Table 2. The solid squares are results of the relativistic LDA calculations.

M R S Internet Journal of Nitride Semiconductor Research

https://doi.org/10.1557/S1092578300002027 Published online by Cambridge University Press